

Generating stable spin squeezing by squeezed-reservoir engineering

Si-Yuan Bai¹ and Jun-Hong An^{1,*}

¹*Lanzhou Center for Theoretical Physics, Key Laboratory of Theoretical Physics of Gansu Province, Lanzhou University, Lanzhou 730000, China*

(Dated: March 1, 2025)

As one kind of many-body entanglement, spin squeezing (SS) has a wide application in practical quantum technology. Its generation has attracted much attention in recent years. It was reported that N two-level systems (TLSs) located near a one-dimensional waveguide can generate a SS by using the mediation effect of the waveguide. However, a coherent driving on each TLS is used to stabilize the SS, which raises a high requirement to experiments. We here propose a scheme to generate stable SS without resorting to the coherent driving on the TLSs. Incorporating the mediation role of the common waveguide and the technique of squeezed-reservoir engineering, our scheme exhibits the advantages over previous ones in the scaling relation of the SS parameter with the number of the TLSs. The long-range correlation feature of the generated SS along the waveguide may endow it certain superiority in quantum sensing, e.g., improving the sensing efficiency of spatially unidentified weak magnetic field.

Introduction.— A quantum-science revolution is in the making. It is expected to bring a lot of profound impacts on technological innovations. A distinguished example is quantum metrology or sensing [1, 2]. It pursues to develop measurement protocols with higher precisions to physical quantities than the limit constrained by classical physics, i.e., the shot-noise limit, by using quantum resources. As a kind of many-body entanglement [3–6], spin squeezing (SS) is one of such resources. It has exhibited a wonderful power in beating the shot noise limit [7–13], with promising applications in quantum gyroscope [14, 15], atomic clocks [16–20], magnetometers [21, 22], and gravimetry [23]. Its efficient generation is a prerequisite for further applications. The widely used method exploits the coherent spin-spin coupling in the one- and two-axis twisting models [4, 7–10, 24]. However, it is dynamically transient and experiences a degradation under the realistic decoherence [25–27]. Other methods via atom-photon couplings [28–30] and quantum nondemolition measurements [31–33] have also been proposed.

Waveguide quantum electrodynamics (QED) refers to a scenario where arrays of quantum emitters coupled to a waveguide [34–41]. It allows for long-range interactions among the quantum emitters mediated by photons in the waveguide that is particularly interesting for quantum network applications [42]. Several schemes on dissipative preparation of the SS [43–50] have been proposed based on the idea of reservoir engineering [51–55] to the waveguide modes. The SS generated in such method exists in steady states and does not depend on initial states, which endows it the features of a long lifetime and robustness. However, a coherent driving laser on each quantum emitters is needed to stabilize the SS in these schemes. It dramatically increases the experimental difficulties when a huge number of quantum emitters are involved.

In this work, we propose a scheme to deterministically generate a stable SS of N distant quantum emitters formed by two-level systems (TLSs) in a waveguide

QED system without resorting to a coherent driving on each TLS. The main idea is based on the combined action of the technique of squeezed-reservoir engineering, which is widely used in quantum state preparation [56–61], and the mediation role of the waveguide. The waveguide enables us to manipulate the phase difference between the reservoir-induced long-range coherent and incoherent couplings of TLSs such that an effective collective spin mode of TLSs is induced by precisely controlling the positions of TLSs. Then, acting as a mold, the squeezed reservoir imprints its squeezing feature to the steady state of the collective spin. It is found that the Wineland SS parameter ξ_R^2 , as a characterization of the improvement of sensitivity in Ramsey spectroscopy [3], for our generated SS scales with the TLS number N as $1.64N^{-0.54}$, which beats the ones in the one- and two-axis twisting [25–27] and Heisenberg [62] models with the realistic dissipation considered. It implies the superiority of the SS of our scheme in quantum sensing. The spatial separation of the TLSs along the waveguide in our scheme also is helpful in improving the sensing efficiency of weak field via effectively increasing the contact area.

System and dynamics.— We consider an array of N equally spaced TLSs as quantum emitters interacting with a common electromagnetic field in a waveguide [see Fig. 1(a)]. The TLSs can be superconductor qubits [63], nitrogen vacancy centers [64], or natural atoms [65]. The waveguide may be a rectangular hollow metal [44], a metal-dielectric surface plasmon [46, 66], or an optical lattice [65]. Its Hamiltonian is $\hat{H} = \hat{H}_S + \hat{H}_R + \hat{H}_I$ with ($\hbar = 1$)

$$\hat{H}_S = \sum_{i=1}^N \omega_0 \hat{\sigma}_i^\dagger \hat{\sigma}_i, \quad \hat{H}_R = \sum_k \omega_k \hat{a}_k^\dagger \hat{a}_k, \quad (1)$$

$$\hat{H}_I = \sum_{k,i} (g_{ki} \hat{a}_k + g_{ki}^* \hat{a}_k^\dagger) (\hat{\sigma}_i^\dagger + \hat{\sigma}_i), \quad (2)$$

where $\hat{\sigma}_i$ is the transition operator from the excited state

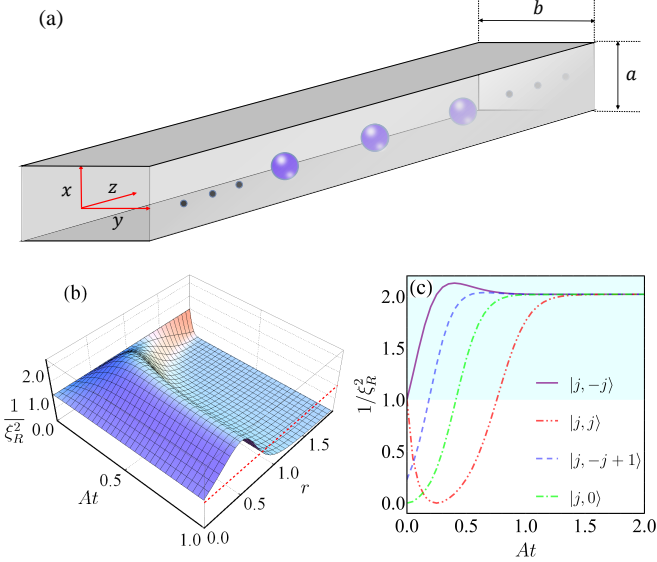


FIG. 1. (a) Schematics of N equally spaced TLSs along z axis in a one-dimensional waveguide, which is driven by a broadband squeezed field. Evolution of the inverse of SS parameter of the TLSs in different r when the initial state is $|j, -j\rangle$ with $j = N/2$ (b) and in different initial states when $r = 0.5$ (c). Other parameters are $N = 10$, $\omega_0 = \Delta = 1.0A$, and $\alpha = 0.5$.

$|e\rangle$ to the ground state $|g\rangle$ of the i th TLS, with transition frequency ω_0 , placed at \mathbf{r}_i and \hat{a}_k is the annihilation operator of the k th mode with frequency ω_k of the reservoir. Their coupling strength is $g_{ki} = \sqrt{\omega_k/(2\epsilon_0)} \mathbf{d}_i \cdot \mathbf{u}_k(\mathbf{r}_i)$, where ϵ_0 is the vacuum permittivity, \mathbf{d}_i is the electric dipole moment of the i th TLS, and $\mathbf{u}_k(\mathbf{r}_i)$ is the spatial function of the k th mode of the reservoir.

We resort to the technique of squeezed-reservoir engineering [57–61] to generate the stable SS of TLSs. It is realized by feeding into the waveguide a broadband squeezed field, which can be implemented via an optical parametric amplification [67]. The electromagnetic field in the waveguide under the driving of the squeezed field acts as a squeezed vacuum reservoir. The initial state of total system reads $\rho_T(0) = \rho(0) \otimes \prod_k \hat{S}_k |0_k\rangle \langle 0_k| \hat{S}_k^\dagger$, where $\hat{S}_k = \exp[(\xi^* \hat{a}_k^2 - \xi \hat{a}_k^{\dagger 2})/2]$ is the squeezing operator with r and α being the squeezing strength and angle, and $|0_k\rangle$ is vacuum state of the k th reservoir mode [56]. We can derive the master equation of the TLSs under the Born-Markovian and secular approximations as [68–70]

$$\begin{aligned} \dot{\rho}(t) = & -i [\Delta_N \sum_i \hat{\sigma}_i^\dagger \hat{\sigma}_i + \hat{H}_{\text{DD}}, \tilde{\rho}(t)] \\ & + \sum_{i,j} \{ \gamma_{ij}^-/2 [\mathcal{N} \check{\mathcal{D}}_{\hat{\sigma}_i^\dagger, \hat{\sigma}_j} + (\mathcal{N}+1) \check{\mathcal{D}}_{\hat{\sigma}_i, \hat{\sigma}_j^\dagger}] \\ & - \gamma_{ij}^+/2 [\mathcal{M} \check{\mathcal{D}}_{\hat{\sigma}_i^\dagger, \hat{\sigma}_j^\dagger} + \mathcal{M}^* \check{\mathcal{D}}_{\hat{\sigma}_i, \hat{\sigma}_j}] \} \tilde{\rho}(t), \end{aligned} \quad (3)$$

where $\tilde{\rho}(t) = e^{i\hat{H}_{\text{st}}} \rho(t) e^{-i\hat{H}_{\text{st}}}$ is the density matrix of TLSs in the interaction picture, $\mathcal{N} \equiv \sinh^2 r$, $\mathcal{M} \equiv \sqrt{\mathcal{N}^2 + \mathcal{N}} e^{i\alpha}$, and $\check{\mathcal{D}}_{\hat{A}, \hat{B}} \equiv 2\hat{A} \cdot \hat{B} - \hat{B}\hat{A} - \hat{B}\hat{A}$. The

first term of Eq. (3) represents the coherent dynamics induced by the reservoir, where $H_{\text{DD}} = -\sum_{i \neq j} \Delta_{ij} (\hat{\sigma}_i^\dagger \hat{\sigma}_j + \hat{\sigma}_i \hat{\sigma}_j^\dagger)/2$ is the reservoir-induced dipole-dipole interaction of the TLSs. The interaction strengths are $\Delta_{ij} = \Delta_{ij}^- + \Delta_{ij}^+$ with $\Delta_{ij}^\pm = \mathcal{P} \int_0^\infty d\omega G_{ij}^\pm(\omega)/(\omega \pm \omega_0)$, where \mathcal{P} denotes the Cauchy principal value and $G_{ij}^-(\omega) \equiv \sum_k g_{ki} g_{kj}^* \delta(\omega - \omega_k)$ are the correlated spectral densities. The frequency shift of each TLS equals to $\Delta_N \equiv (2\mathcal{N}+1)\Delta$ with $\Delta = (\Delta_{ii}^+ - \Delta_{ii}^-)$, which is independent of the positions of TLSs. The second and third lines of Eq. (3) describe the incoherent dissipation and squeezing induced by the reservoir, respectively. The dissipation and squeezing rates read $\gamma_{ij}^\pm = 2\pi G_{ij}^\pm(\omega_0)$, with $G_{ij}^+(\omega) \equiv \sum_k g_{ki} g_{kj} \delta(\omega - \omega_j)$. It is interesting to see that the waveguide, as a common medium of the TLSs to confine the squeezed vacuum field, can not only induce individual dissipation, squeezing, and frequency shift to each TLSs, but also induce correlated dissipation, squeezing, and coherent dipole-dipole interactions to the TLSs by the exchange of virtual photons. This gives us a sufficient room to generate a long-range correlation of TLSs via engineering the reservoir in the waveguide.

For concreteness, we consider that the waveguide is formed by a rectangular hollow metal. The electromagnetic modes in the waveguide are the transverse modes TE_{mn} and TM_{mn} with the cutoff frequency $\omega_{mn} = c[(m\pi/a)^2 + (n\pi/b)^2]^{1/2}$, where a, b are the transverse lengths of the waveguide, and m, n are non-negative integers. Their dispersion relations are $\omega_k^{mn} = [(ck)^2 + \omega_{mn}^2]^{1/2}$ with k being the longitudinal wave number and c being the speed of light [71]. Assuming that the TLSs are polarized in the z direction ($\mathbf{d}_i = d\mathbf{e}_z$), we can calculate the spectral densities as [44]

$$G_{ij}^\pm(\omega) = \sum_{mn} \frac{\Gamma_{mn}}{2\pi} \frac{\cos[k(z_i \pm z_j)]}{[(\omega/\omega_{mn})^2 - 1]^{1/2}} \Theta(\omega - \omega_{mn}) \quad (4)$$

with $\Theta(\omega - \omega_{mn})$ being the Heaviside step function, $\Gamma_{mn} = 4\omega_{mn} \tilde{u}_{mn,i} \tilde{u}_{mn,j}/(\epsilon_0 c a b)$, and $\tilde{u}_{mn,i} = d \sin(\frac{m\pi}{a} x_i) \sin(\frac{n\pi}{b} y_i)$.

We consider only the dominated mode with $m = n = 1$. Focusing on $\omega_0 > \omega_{11}$ and using the Cauchy's residue theorem [72], we can readily derive [70]

$$\Delta_{ij} = -[\Gamma_{11} \zeta \omega_{11}/(2c)] \sin(|z_i - z_j|/\zeta), \quad (5)$$

$$\gamma_{ij}^\pm = (\Gamma_{11} \zeta \omega_{11}/c) \cos(|z_i \pm z_j|/\zeta), \quad (6)$$

where $\zeta = c(\omega_0^2 - \omega_{11}^2)^{-1/2}$. The distance-dependent terms in Eqs. (5) and (6) originate from the interference of the N individual interaction channels of the TLSs with the common squeezed reservoir in the waveguide [73]. As a remarkable feature, the waveguide as the environment medium enables us to modulate the phase difference between the waveguide-mediated coherent and incoherent couplings of the TLSs via tailoring their position z_i . This might allow the switch-on/off either of the two couplings

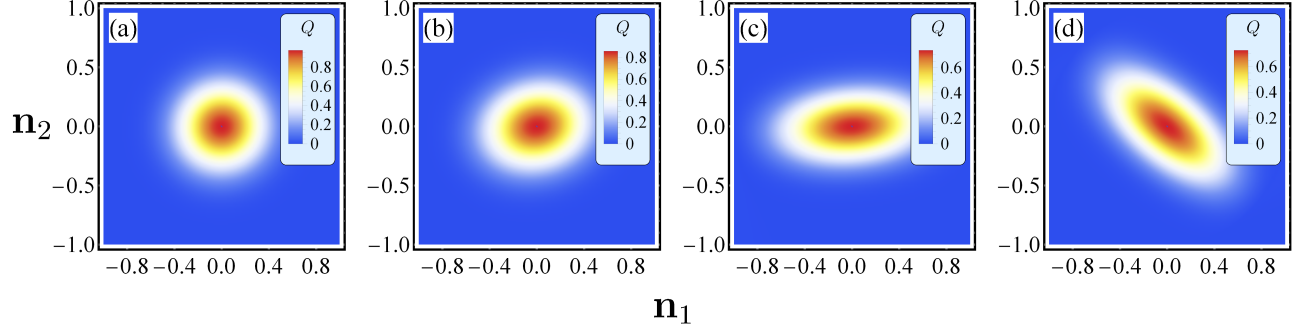


FIG. 2. Evolution of the Husimi's Q function in the plane \mathbf{n}_\perp for the initial state $|j, -j\rangle$ when $t = 0$ in (a), $0.01A^{-1}$ in (b), $0.1A^{-1}$ in (c), and $t = 4.0A^{-1}$ in (d). We use $N = 30$, $r = 0.8$, and the others being the same as Fig. 1.

and offer an opportunity for engineering the multipartite quantum correlation of the TLSs. By precisely positioning the TLSs such that $|z_i \pm z_j| = 2n_\pm\pi\zeta$ ($n_\pm \in \mathbb{Z}$), we have $\gamma_{ij}^\pm = \Gamma_{11}\zeta\omega_{11}/c \equiv A$ and $\Delta_{ij} = 0$. Equation (3) is reduced to a form of collective spin as [70]

$$\dot{\rho}(t) = -i\Delta_N[\hat{S}^z, \tilde{\rho}(t)] + \frac{A}{2} \left[\mathcal{N}\check{\mathcal{D}}_{\hat{S}^+, \hat{S}^-} + (\mathcal{N}+1)\check{\mathcal{D}}_{\hat{S}^-, \hat{S}^+} - \mathcal{M}\check{\mathcal{D}}_{\hat{S}^+, \hat{S}^+} - \mathcal{M}^*\check{\mathcal{D}}_{\hat{S}^-, \hat{S}^-} \right] \tilde{\rho}(t), \quad (7)$$

where $\hat{S}^z \equiv \sum_i (\hat{\sigma}_i^\dagger \hat{\sigma}_i - 1/2)$ and $\hat{S}^- = (\hat{S}^+)^{\dagger} = \sum_i \hat{\sigma}_i$. Thus, the individual behavior disappears and only the collective behavior of the TLSs is manifested due to the constructive interference among the interaction channels.

Spin squeezing in steady state.— A SS characterizes the reduced quantum fluctuation in certain spin component. Any spin state ρ defines a mean spin direction $\mathbf{n} = \text{Tr}(\hat{\mathbf{S}}\rho)/|\text{Tr}(\hat{\mathbf{S}}\rho)| \equiv (\sin\theta_0 \cos\varphi_0, \sin\theta_0 \sin\varphi_0, \cos\theta_0)$, where θ_0 and φ_0 are the polar and azimuthal angles of $\text{Tr}(\rho\hat{\mathbf{S}})$. It is squeezed if the minimal variance of the spin component in the perpendicular plane \mathbf{n}_\perp spanned by $\mathbf{n}_1 = (\cos\theta_0 \cos\varphi_0, \cos\theta_0 \sin\varphi_0, -\sin\theta_0)$ and $\mathbf{n}_2 = (-\sin\varphi_0, \cos\varphi_0, 0)$ is smaller than the one of the spin coherent state associated with \mathbf{n} , which equals to $N/4$ [4]. It is quantified by the SS parameter [3]

$$\xi_R^2 = \left(\frac{N/2}{|\text{Tr}(\hat{\mathbf{S}}\rho)|} \right)^2 \frac{[\text{Var}(\hat{\mathbf{S}}^\perp)]_{\text{min}}}{N/4} = \frac{N[\text{Var}(\hat{\mathbf{S}}^\perp)]_{\text{min}}}{|\text{Tr}(\hat{\mathbf{S}}\rho)|^2}, \quad (8)$$

where $\hat{\mathbf{S}}^\perp$ is the spin vector in the plane of \mathbf{n}_\perp , the operator variance is defined as $\text{Var}(\hat{O}) = \langle \hat{O}^2 \rangle - \langle \hat{O} \rangle^2$, and the superscript min means the minimum in all allowable directions. Exhibiting multipartite entanglement, the state is squeezed when $\xi_R^2 < 1$ [74]. Another widely used way to visually depict the SS is the Husimi's Q function defined as $Q(\theta, \varphi) = (2j+1)/(4\pi) \langle \theta, \varphi | \rho | \theta, \varphi \rangle$ [75], where $|\theta, \varphi\rangle = (1 + |\eta|^2)^{-j} e^{-\eta^* \hat{S}^-} |j, j\rangle$ with $|j, m\rangle$ ($m = -j, \dots, j$) being the common eigenstates of $\{\hat{\mathbf{S}}^2, \hat{S}^z\}$ and $\eta = -\tan(\theta/2)e^{-i\varphi}$. The Q function is centered at \mathbf{n} on the Bloch sphere. It succeeds in mapping the density

matrix ρ to a quasi-classical probability distribution in the phase space defined by θ and φ .

Via numerically solving the master equation (7), we show in Fig. 1(b) the time evolution of $1/\xi_R^2$ for the initial state $|j, -j\rangle$ with $j = N/2$ in different squeezing strengths r of the reservoir. It can be found that a stable SS can be formed in the regime of a moderate squeezing strength r . Thanks to the constructive role played by the squeezed reservoir in the waveguide, the system spontaneously evolves to a spin squeezed state uniquely dependent on r . This is in sharp contrast to the previous results [46–50], where a coherent driving field is applied on each TLS to stabilize the SS. Figure 1(c) gives the evolution of $1/\xi_R^2$ with chosen r in different initial states $|j, m\rangle$. It verifies the uniqueness of the steady state. We plot in Fig. 2 the evolution of the projections of Q function in the \mathbf{n}_\perp plane for the initial state $|j, -j\rangle$. Being isotropically distributed, it shows no SS in the initial state. With increasing the evolution time, it keeps shrinking in one direction at the expense of expanding in its orthogonal direction. Such SS is kept to its steady state [see Fig. 2(d)]. It confirms our result that the TLSs as a collective spin is squeezed by the squeezed reservoir.

To figure out the relation between the steady-state SS and the squeezing strength r , we calculate the steady state [70, 76]

$$\tilde{\rho}(\infty) = \sum_{m,n=-j}^j p_m p_n^* \langle \phi_m | \phi_n \rangle |\psi_m\rangle \langle \psi_n|. \quad (9)$$

Satisfying $\hat{R}_z|\psi_m\rangle = m|\psi_m\rangle$ and $\hat{R}_z^\dagger|\phi_m\rangle = m|\phi_m\rangle$ with $\hat{R}_z = i(4|\mathcal{M}|)^{-1/2}(\hat{S}^+ e^{i\frac{\alpha}{2}} \sinh r - \hat{S}^- e^{-i\frac{\alpha}{2}} \cosh r)$, $|\psi_m\rangle$ and $|\phi_m\rangle$ form a complete set of biorthogonal basis. The recurrence relation of coefficient p_m is

$$p_{m+1} = \frac{Am - i\Delta_N}{A(m+1) + i\Delta_N} p_m, \quad (10)$$

which can be fixed by $\text{Tr}[\tilde{\rho}(\infty)] = 1$.

We plot in Fig. 3(a) the comparison of the steady-state squeezing obtained by the analytical solution (9) with the

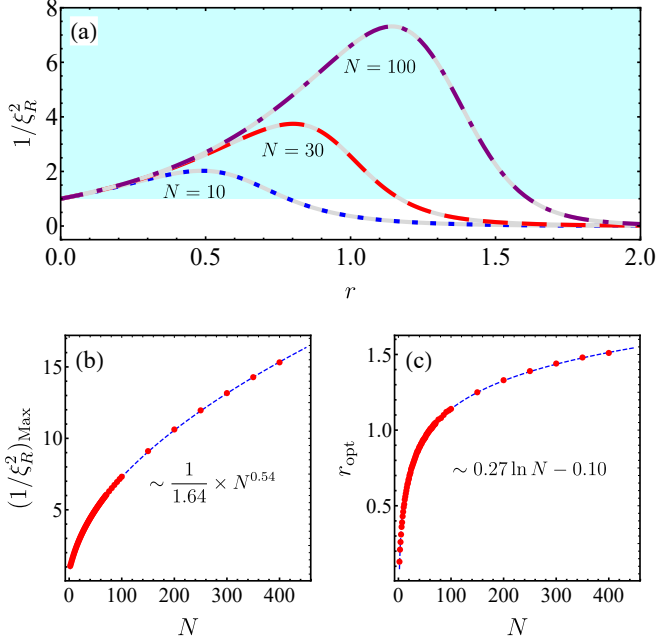


FIG. 3. (a) Comparison of $1/\xi_R^2$ obtained by the analytical solution (9) (purple dot-dashed, red dashed, and blue dotted lines) with the one by numerically solving Eq. (7) at $t = 200A^{-1}$ (gray lines) in different N . Maxima of $1/\xi_R^2$ (b) and optimal r (c) as function of N , which are numerically fitted as $(\xi_R^2)_{\text{Max}} = 1.64N^{-0.54}$ and $r_{\text{opt}} = 0.27 \ln N - 0.1$, respectively. Other parameters are the same as Fig. 2.

one by numerically solving Eq. (7). It shows that the analytical result matches with the numerical one, which verifies the correctness of Eq. (9) in describing the steady state of our system. An observation from Fig. 3(a) is that the SS sensitively depends on the squeezing strength r . With increasing the number N of the TLSs, the range of r supporting the stable SS becomes wider and wider. Thus, the stable SS can be generated in a fairly wider parameter range if more TLSs are involved. It is noticed that, even for sufficiently large N , the SS still tends to vanish in gradual manner with the increase of r . This is different from the previous schemes based on driven-dissipative Dicke model [46, 49], where a nonequilibrium phase transition manifested by an abrupt change of the steady-state SS presents. It is understandable based on the fact that the SS in our scheme is generated via purely incoherent interactions of TLSs mediated by the reservoir, while theirs is via the combined actions of the incoherent interactions and coherent driving.

Besides characterizing the many-body entanglement, the SS parameter ξ_R^2 also describes the improvement of the sensitivity to measure the atomic frequency in Ramsey spectroscopy [3]. Therefore, it itself is an important quantity to characterize quantum superiority in quantum metrology [77–80]. The analytical solution (9) permits us to investigate the SS in the large- N limit, where the numerical calculation is hard. The relation between the

optimal SS we can achieve and the number N of the TLSs are calculated via Eq. (9) [see red dots in Fig. 3(b)]. Via numerical fitting, we obtain its scaling relation as

$$(\xi_R^2)_{\text{Min}} = 1.64 \times N^{-0.54}. \quad (11)$$

According to the definition of ξ_R^2 [3], the metrology error using this state in the frequency estimation of Ramsey spectroscopy outperforms the shot-noise limit achieved by the spin coherent by a factor $\sqrt{1.64}N^{-0.27}$. Such performance is better than the previous schemes. For comparison, the SS generated via the coherent one-axis twisting scales as $\xi_R^2 \propto N^{-2/3}$ and via two-axis twisting as N^{-1} in the ideal situation [4]. However, they tend to $N^{-1/2}$ at optimized time and to be divergent in the long-time limit when the dissipation is considered [25–27]. The SS in our system is also better than the one in the ground state of Lipkin-Meshkov-Glick model scaling as $\xi_R^2 \propto N^{-1/3}$ [81] and the one in the steady state of dissipative anisotropic Heisenberg model scaling as $\xi_R^2 = 1/2$ [62]. Figure 3(c) shows the squeezing strength of the reservoir we need to obtain the best SS in different N . The numerical fitting reveals that it scales with N as $r_{\text{opt}} = 0.27 \ln N - 0.1$, which shows a gentle dependence with N . It means that we are not bothered to sharply increase r in order to generate the SS for a large number of TLSs. This gives a useful guideline for experiments to optimizing the working condition.

Discussion and conclusion.— The current experimental advance in fabricating nanophotonic waveguide provides a technical support to our scheme [35–39]. The transmission-line waveguide mediated interactions of two 18.6 mm separated TLSs have been observed [35]. A 15 dB squeezed light corresponding to squeezing strength $r = 1.7$ has been realized [82], which fulfills our requirement. The precise positioning of TLSs in a 20-nm accuracy has been realized [83, 84]. Our scheme can also be realized in SiV centers as TLSs in a diamond waveguide [38, 42, 54, 85]. Comparing with the SS in atom ensemble [7–13], the SS in our scheme shows a long-range correlation. This feature hopefully is useful in developing quantum sensing strategy in extremal condition, e.g., improving the sensing efficiency of spatially unidentified weak magnetic field via effectively increasing the contact area.

In summary, we have proposed a scheme to generate stable SS of N distant TLSs in a waveguide QED system by squeezed-reservoir engineering. A collective effect of the far separated TLSs is efficiently created by the mediation role of the common squeezed reservoir in the waveguide via well designing the positions of TLSs. It makes the TLSs spontaneously evolves from any initial state to a spin squeezed state in the long-time limit. Our analysis reveals that the generated SS scales with the number of TLSs as $N^{-0.54}$, which shows an advantage over the two-axis twisting and Heisenberg models with the realistic dissipation considered. Without resorting

to the coherent driving on each TLSs, our scheme reduces the difficulty of experiment realization in previous schemes. The recent advance of the waveguide QED experiments indicates that our scheme is within the present experimental state of the art.

Acknowledgments.— The work is supported by the National Natural Science Foundation (Grants No. 11875150, No. 11834005, and No. 12047501).

* anjhong@lzu.edu.cn

[1] C. L. Degen, F. Reinhard, and P. Cappellaro, “Quantum sensing,” *Rev. Mod. Phys.* **89**, 035002 (2017).

[2] Luca Pezzè, Augusto Smerzi, Markus K. Oberthaler, Roman Schmied, and Philipp Treutlein, “Quantum metrology with nonclassical states of atomic ensembles,” *Rev. Mod. Phys.* **90**, 035005 (2018).

[3] D. J. Wineland, J. J. Bollinger, W. M. Itano, F. L. Moore, and D. J. Heinzen, “Spin squeezing and reduced quantum noise in spectroscopy,” *Phys. Rev. A* **46**, R6797–R6800 (1992).

[4] Masahiro Kitagawa and Masahito Ueda, “Squeezed spin states,” *Phys. Rev. A* **47**, 5138–5143 (1993).

[5] Bernd Lücke, Jan Peise, Giuseppe Vitagliano, Jan Arlt, Luis Santos, Géza Tóth, and Carsten Klempert, “Detecting multiparticle entanglement of dicke states,” *Phys. Rev. Lett.* **112**, 155304 (2014).

[6] Jian Ma, Xiaoguang Wang, C.P. Sun, and Franco Nori, “Quantum spin squeezing,” *Physics Reports* **509**, 89–165 (2011).

[7] Justin G Bohnet, Kevin C Cox, Matthew A Norcia, Joshua M Weiner, Zilong Chen, and James K Thompson, “Reduced spin measurement back-action for a phase sensitivity ten times beyond the standard quantum limit,” *Nature Photonics* **8**, 731–736 (2014).

[8] Justin G. Bohnet, Brian C. Sawyer, Joseph W. Britton, Michael L. Wall, Ana Maria Rey, Michael Foss-Feig, and John J. Bollinger, “Quantum spin dynamics and entanglement generation with hundreds of trapped ions,” *Science* **352**, 1297–1301 (2016).

[9] O. Hosten, R. Krishnakumar, N. J. Engelsen, and M. A. Kasevich, “Quantum phase magnification,” *Science* **352**, 1552–1555 (2016).

[10] Onur Hosten, Nils J Engelsen, Rajiv Krishnakumar, and Mark A Kasevich, “Measurement noise 100 times lower than the quantum-projection limit using entangled atoms,” *Nature* **529**, 505–508 (2016).

[11] Xin-Yu Luo, Yi-Quan Zou, Ling-Na Wu, Qi Liu, Ming-Fei Han, Meng Khoon Tey, and Li You, “Deterministic entanglement generation from driving through quantum phase transitions,” *Science* **355**, 620–623 (2017).

[12] Yi-Quan Zou, Ling-Na Wu, Qi Liu, Xin-Yu Luo, Shuai-Feng Guo, Jia-Hao Cao, Meng Khoon Tey, and Li You, “Beating the classical precision limit with spin-1 Dicke states of more than 10,000 atoms,” *Proceedings of the National Academy of Sciences* **115**, 6381 (2018).

[13] Han Bao, Junlei Duan, Shenchao Jin, Xingda Lu, Pengxiong Li, Weizhi Qu, Mingfeng Wang, Irina Novikova, Eugeniy E. Mikhailov, Kai-Feng Zhao, Klaus Mølmer, Heng Shen, and Yanhong Xiao, “Spin squeezing of 10^{11} atoms by prediction and retrodiction measurements,” *Nature (London)* **581**, 159 (2020).

[14] G.-B. Jo, Y. Shin, S. Will, T. A. Pasquini, M. Saba, W. Ketterle, D. E. Pritchard, M. Vengalattore, and M. Prentiss, “Long phase coherence time and number squeezing of two Bose-Einstein condensates on an atom chip,” *Phys. Rev. Lett.* **98**, 030407 (2007).

[15] P. Berg, S. Abend, G. Tackmann, C. Schubert, E. Giese, W. P. Schleich, F. A. Narducci, W. Ertmer, and E. M. Rasel, “Composite-light-pulse technique for high-precision atom interferometry,” *Phys. Rev. Lett.* **114**, 063002 (2015).

[16] Ian D. Leroux, Monika H. Schleier-Smith, and Vladan Vuletić, “Orientation-dependent entanglement lifetime in a squeezed atomic clock,” *Phys. Rev. Lett.* **104**, 250801 (2010).

[17] E. M. Kessler, P. Kómár, M. Bishof, L. Jiang, A. S. Sørensen, J. Ye, and M. D. Lukin, “Heisenberg-limited atom clocks based on entangled qubits,” *Phys. Rev. Lett.* **112**, 190403 (2014).

[18] P. Kómár, E. M. Kessler, M. Bishof, L. Jiang, A. S. Sørensen, J. Ye, and M. D. Lukin, “A quantum network of clocks,” *Nature Physics* **10**, 582–587 (2014).

[19] I. Kruse, K. Lange, J. Peise, B. Lücke, L. Pezzè, J. Arlt, W. Ertmer, C. Lisdat, L. Santos, A. Smerzi, and C. Klempert, “Improvement of an atomic clock using squeezed vacuum,” *Phys. Rev. Lett.* **117**, 143004 (2016).

[20] Edwin Pedrozo-Peñaflor, Simone Colombo, Chi Shu, Albert F. Adiyatullin, Zeyang Li, Enrique Mendez, Boris Braverman, Akio Kawasaki, Daisuke Akamatsu, Yanhong Xiao, and Vladan Vuletić, “Entanglement on an optical atomic-clock transition,” *Nature* **588**, 414–418 (2020).

[21] R. J. Sewell, M. Koschorreck, M. Napolitano, B. Dubost, N. Behbood, and M. W. Mitchell, “Magnetic sensitivity beyond the projection noise limit by spin squeezing,” *Phys. Rev. Lett.* **109**, 253605 (2012).

[22] W. Muessel, H. Strobel, D. Linnemann, D. B. Hume, and M. K. Oberthaler, “Scalable spin squeezing for quantum-enhanced magnetometry with Bose-Einstein condensates,” *Phys. Rev. Lett.* **113**, 103004 (2014).

[23] Stuart S. Szigeti, Samuel P. Nolan, John D. Close, and Simon A. Haine, “High-precision quantum-enhanced gravimetry with a Bose-Einstein condensate,” *Phys. Rev. Lett.* **125**, 100402 (2020).

[24] Y. C. Liu, Z. F. Xu, G. R. Jin, and L. You, “Spin squeezing: Transforming one-axis twisting into two-axis twisting,” *Phys. Rev. Lett.* **107**, 013601 (2011).

[25] Anders Søndberg Sørensen and Klaus Mølmer, “Entangling atoms in bad cavities,” *Phys. Rev. A* **66**, 022314 (2002).

[26] Xiaoguang Wang, Adam Miranowicz, Yu-xi Liu, C. P. Sun, and Franco Nori, “Sudden vanishing of spin squeezing under decoherence,” *Phys. Rev. A* **81**, 022106 (2010).

[27] Peng Xue, “Non-Markovian dynamics of spin squeezing,” *Physics Letters A* **377**, 1328–1332 (2013).

[28] Yong-Chang Zhang, Xiang-Fa Zhou, Xingxiang Zhou, Guang-Can Guo, and Zheng-Wei Zhou, “Cavity-assisted single-mode and two-mode spin-squeezed states via phase-locked atom-photon coupling,” *Phys. Rev. Lett.* **118**, 083604 (2017).

[29] Stuart J. Masson and Scott Parkins, “Rapid production of many-body entanglement in spin-1 atoms via cavity output photon counting,” *Phys. Rev. Lett.* **122**, 103601

(2019).

[30] Peter Groszkowski, Hoi-Kwan Lau, C. Leroux, L. C. G. Govia, and A. A. Clerk, “Heisenberg-limited spin squeezing via bosonic parametric driving,” *Phys. Rev. Lett.* **125**, 203601 (2020).

[31] A. Kuzmich, L. Mandel, and N. P. Bigelow, “Generation of spin squeezing via continuous quantum nondemolition measurement,” *Phys. Rev. Lett.* **85**, 1594–1597 (2000).

[32] J. Appel, P. J. Windpassinger, D. Oblak, U. B. Hoff, N. Kjærgaard, and E. S. Polzik, “Mesoscopic atomic entanglement for precision measurements beyond the standard quantum limit,” *Proceedings of the National Academy of Sciences* **106**, 10960–10965 (2009).

[33] Michail Kritsotakis, Jacob A. Dunningham, and Simon A. Haine, “Spin squeezing of a Bose-Einstein condensate via a quantum nondemolition measurement for quantum-enhanced atom interferometry,” *Phys. Rev. A* **103**, 023318 (2021).

[34] T. Lund-Hansen, S. Stobbe, B. Julsgaard, H. Thyrrstrup, T. Sünder, M. Kamp, A. Forchel, and P. Lodahl, “Experimental realization of highly efficient broadband coupling of single quantum dots to a photonic crystal waveguide,” *Phys. Rev. Lett.* **101**, 113903 (2008).

[35] Arjan F. van Loo, Arkady Fedorov, Kevin Lalumière, Barry C. Sanders, Alexandre Blais, and Andreas Wallraff, “Photon-mediated interactions between distant artificial atoms,” *Science* **342**, 1494–1496 (2013).

[36] Jan Petersen, Jürgen Volz, and Arno Rauschenbeutel, “Chiral nanophotonic waveguide interface based on spin-orbit interaction of light,” *Science* **346**, 67–71 (2014).

[37] R. Mitsch, C. Sayrin, B. Albrecht, P. Schneeweiss, and A. Rauschenbeutel, “Quantum state-controlled directional spontaneous emission of photons into a nanophotonic waveguide,” *Nature Communications* **5**, 5713 (2014).

[38] A. Sipahigil, R. E. Evans, D. D. Sukachev, M. J. Burek, J. Borregaard, M. K. Bhaskar, C. T. Nguyen, J. L. Pacheco, H. A. Atikian, C. Meuwly, R. M. Camacho, F. Jelezko, E. Bielejec, H. Park, M. Lončar, and M. D. Lukin, “An integrated diamond nanophotonics platform for quantum-optical networks,” *Science* **354**, 847–850 (2016).

[39] Bharath Kannan, Max J. Ruckriegel, Daniel L. Campbell, Anton Frish Kockum, Jochen Braumüller, David K. Kim, Morten Kjaergaard, Philip Krantz, Alexander Melville, Bethany M. Niedzielski, Antti Vepsäläinen, Roni Winik, Jonilyn L. Yoder, Franco Nori, Terry P. Orlando, Simon Gustavsson, and William D. Oliver, “Waveguide quantum electrodynamics with superconducting artificial giant atoms,” *Nature (London)* **583**, 775–779 (2020).

[40] B. Kannan, D. L. Campbell, F. Vasconcelos, R. Winik, D. K. Kim, M. Kjaergaard, P. Krantz, A. Melville, B. M. Niedzielski, J. L. Yoder, T. P. Orlando, S. Gustavsson, and W. D. Oliver, “Generating spatially entangled itinerant photons with waveguide quantum electrodynamics,” *Science Advances* **6**, eabb8780 (2020).

[41] Eunjong Kim, Xueyue Zhang, Vinicius S. Ferreira, Jash Bunker, Joseph K. Iverson, Alp Sipahigil, Miguel Bello, Alejandro González-Tudela, Mohammad Mirhosseini, and Oskar Painter, “Quantum electrodynamics in a topological waveguide,” *Phys. Rev. X* **11**, 011015 (2021).

[42] M.-A. Lemonde, S. Meesala, A. Sipahigil, M. J. A. Schuetz, M. D. Lukin, M. Loncar, and P. Rabl, “Phonon networks with silicon-vacancy centers in diamond waveguides,” *Phys. Rev. Lett.* **120**, 213603 (2018).

[43] Hanna Krauter, Christine A. Muschik, Kasper Jensen, Wojciech Wasilewski, Jonas M. Petersen, J. Ignacio Cirac, and Eugene S. Polzik, “Entanglement generated by dissipation and steady state entanglement of two macroscopic objects,” *Phys. Rev. Lett.* **107**, 080503 (2011).

[44] Ephraim Shahmoon and Gershon Kurizki, “Nonradiative interaction and entanglement between distant atoms,” *Phys. Rev. A* **87**, 033831 (2013).

[45] A. Gonzalez-Tudela, D. Martin-Cano, E. Moreno, L. Martin-Moreno, C. Tejedor, and F. J. Garcia-Vidal, “Entanglement of two qubits mediated by one-dimensional plasmonic waveguides,” *Phys. Rev. Lett.* **106**, 020501 (2011).

[46] Alejandro González-Tudela and Diego Porras, “Mesoscopic entanglement induced by spontaneous emission in solid-state quantum optics,” *Phys. Rev. Lett.* **110**, 080502 (2013).

[47] A. González-Tudela, V. Paulisch, D. E. Chang, H. J. Kimble, and J. I. Cirac, “Deterministic generation of arbitrary photonic states assisted by dissipation,” *Phys. Rev. Lett.* **115**, 163603 (2015).

[48] Emanuele G. Dalla Torre, Johannes Otterbach, Eugene Demler, Vladan Vuletic, and Mikhail D. Lukin, “Dissipative preparation of spin squeezed atomic ensembles in a steady state,” *Phys. Rev. Lett.* **110**, 120402 (2013).

[49] Wanlu Song, Wanli Yang, Junhong An, and Mang Feng, “Dissipation-assisted spin squeezing of nitrogen-vacancy centers coupled to a rectangular hollow metallic waveguide,” *Opt. Express* **25**, 19226–19235 (2017).

[50] Yi-Fan Qiao, Hong-Zhen Li, Xing-Liang Dong, Jia-Qiang Chen, Yuan Zhou, and Peng-Bo Li, “Phononic-waveguide-assisted steady-state entanglement of silicon-vacancy centers,” *Phys. Rev. A* **101**, 042313 (2020).

[51] Daniel Kienzler, H-Y Lo, B Keitch, L de Clercq, F Leupold, F Lindenfelser, M Marinelli, V Negnevitsky, and JP Home, “Quantum harmonic oscillator state synthesis by reservoir engineering,” *Science* , 1261033 (2014).

[52] A. Metelmann and A. A. Clerk, “Nonreciprocal photon transmission and amplification via reservoir engineering,” *Phys. Rev. X* **5**, 021025 (2015).

[53] Harald R. Haakh and Stefan Scheel, “Modified and controllable dispersion interaction in a one-dimensional waveguide geometry,” *Phys. Rev. A* **91**, 052707 (2015).

[54] K. V. Kepesidis, M.-A. Lemonde, A. Norambuena, J. R. Maze, and P. Rabl, “Cooling phonons with phonons: Acoustic reservoir engineering with silicon-vacancy centers in diamond,” *Phys. Rev. B* **94**, 214115 (2016).

[55] Yariv Yanay and Aashish A. Clerk, “Reservoir engineering of bosonic lattices using chiral symmetry and localized dissipation,” *Phys. Rev. A* **98**, 043615 (2018).

[56] J. Roßnagel, O. Abah, F. Schmidt-Kaler, K. Singer, and E. Lutz, “Nanoscale heat engine beyond the carnot limit,” *Phys. Rev. Lett.* **112**, 030602 (2014).

[57] Chun-Jie Yang, Jun-Hong An, Wanli Yang, and Yong Li, “Generation of stable entanglement between two cavity mirrors by squeezed-reservoir engineering,” *Phys. Rev. A* **92**, 062311 (2015).

[58] Sina Zeytinoglu, Ataç İmamoğlu, and Sebastian Hu-

ber, "Engineering matter interactions using squeezed vacuum," *Phys. Rev. X* **7**, 021041 (2017).

[59] S. Kono, Y. Masuyama, T. Ishikawa, Y. Tabuchi, R. Yamazaki, K. Usami, K. Koshino, and Y. Nakamura, "Non-classical photon number distribution in a superconducting cavity under a squeezed drive," *Phys. Rev. Lett.* **119**, 023602 (2017).

[60] Wei Qin, Adam Miranowicz, Peng-Bo Li, Xin-You Lü, J. Q. You, and Franco Nori, "Exponentially enhanced light-matter interaction, cooperativities, and steady-state entanglement using parametric amplification," *Phys. Rev. Lett.* **120**, 093601 (2018).

[61] Stefano Zippilli and David Vitali, "Dissipative engineering of gaussian entangled states in harmonic lattices with a single-site squeezed reservoir," *Phys. Rev. Lett.* **126**, 020402 (2021).

[62] Tony E. Lee, Sarang Gopalakrishnan, and Mikhail D. Lukin, "Unconventional magnetism via optical pumping of interacting spin systems," *Phys. Rev. Lett.* **110**, 257204 (2013).

[63] Yanbing Liu and Andrew A. Houck, "Quantum electrodynamics near a photonic bandgap," *Nature Physics* **13**, 48–52 (2017).

[64] Wanlu Song, Wanli Yang, Junhong An, and Mang Feng, "Dissipation-assisted spin squeezing of nitrogen-vacancy centers coupled to a rectangular hollow metallic waveguide," *Opt. Express* **25**, 19226–19235 (2017).

[65] Ludwig Krinner, Michael Stewart, Arturo Pazmiño, Joonhyuk Kwon, and Dominik Schneble, "Spontaneous emission of matter waves from a tunable open quantum system," *Nature* **559**, 589–592 (2018).

[66] Chun-Jie Yang, Jun-Hong An, and Hai-Qing Lin, "Signatures of quantized coupling between quantum emitters and localized surface plasmons," *Phys. Rev. Research* **1**, 023027 (2019).

[67] Takahiro Serikawa, Jun ichi Yoshikawa, Kenzo Makino, and Akira Frusawa, "Creation and measurement of broadband squeezed vacuum from a ring optical parametric oscillator," *Opt. Express* **24**, 28383–28391 (2016).

[68] Heinz-Peter Breuer and Francesco Petruccione, *The Theory of Open Quantum Systems* (Oxford University Press, Oxford, 2007).

[69] H. Mäkelä and M. Möttönen, "Effects of the rotating-wave and secular approximations on non-Markovianity," *Phys. Rev. A* **88**, 052111 (2013).

[70] See the Supplemental Material for a detailed derivation of the master equation, its reduction to the form of the collective spin, and the steady-state solution.

[71] Jin Au Kong, *Electromagnetic Wave Theory* (John Wiley and Sons, New York, 1986).

[72] Sadri Hassani, *Mathematical Physics: A Modern Introduction to Its Foundations*, 2nd ed. (Springer International Publishing, New York, 2013).

[73] Chong Chen, Chun-Jie Yang, and Jun-Hong An, "Exact decoherence-free state of two distant quantum systems in a non-Markovian environment," *Phys. Rev. A* **93**, 062122 (2016).

[74] Géza Tóth, Christian Knapp, Otfried Gühne, and Hans J. Briegel, "Spin squeezing and entanglement," *Phys. Rev. A* **79**, 042334 (2009).

[75] U. Leonhardt and H. Paul, "Phase measurement and Q function," *Phys. Rev. A* **47**, R2460–R2463 (1993).

[76] G. S. Agarwal and R. R. Puri, "Cooperative behavior of atoms irradiated by broadband squeezed light," *Phys. Rev. A* **41**, 3782–3791 (1990).

[77] Christian Gross, "Spin squeezing, entanglement and quantum metrology with Bose–Einstein condensates," *Journal of Physics B: Atomic, Molecular and Optical Physics* **45**, 103001 (2012).

[78] Géza Tóth and Iagoba Apellaniz, "Quantum metrology from a quantum information science perspective," *Journal of Physics A: Mathematical and Theoretical* **47**, 424006 (2014).

[79] Vittorio Giovannetti, Seth Lloyd, and Lorenzo Maccone, "Advances in quantum metrology," *Nature Photonics* **5**, 222–229 (2011).

[80] Tony E. Lee, Florentin Reiter, and Nimrod Moiseyev, "Entanglement and spin squeezing in non-Hermitian phase transitions," *Phys. Rev. Lett.* **113**, 250401 (2014).

[81] Sébastien Dusuel and Julien Vidal, "Finite-size scaling exponents of the Lipkin-Meshkov-Glick model," *Phys. Rev. Lett.* **93**, 237204 (2004).

[82] Henning Vahlbruch, Moritz Mehmet, Karsten Danzmann, and Roman Schnabel, "Detection of 15 db squeezed states of light and their application for the absolute calibration of photoelectric quantum efficiency," *Phys. Rev. Lett.* **117**, 110801 (2016).

[83] Arun Mohan, Pascal Gallo, Marco Felici, Benjamin Dvir, Alok Rudra, Jerome Faist, and Eli Kapon, "Record-low inhomogeneous broadening of site-controlled quantum dots for nanophotonics," *Small* **6**, 1268–1272 (2010).

[84] Marco Felici, Giorgio Pettinari, Francesco Biccari, Alice Boschetti, Saeed Younis, Simone Birindelli, Massimo Gurioli, Anna Vinattieri, Annamaria Gerardino, Luca Businaro, Mark Hopkinson, Silvia Rubini, Mario Capizzi, and Antonio Polimeni, "Broadband enhancement of light-matter interaction in photonic crystal cavities integrating site-controlled quantum dots," *Phys. Rev. B* **101**, 205403 (2020).

[85] Junfeng Wang, Yu Zhou, Xiaoming Zhang, Fucai Liu, Yan Li, Ke Li, Zheng Liu, Guanzhong Wang, and Weibo Gao, "Efficient generation of an array of single silicon-vacancy defects in silicon carbide," *Phys. Rev. Applied* **7**, 064021 (2017).

Supplemental material for “Generating stable spin squeezing by squeezed-reservoir engineering”

Si-Yuan Bai¹ and Jun-Hong An^{1,*}

¹*Lanzhou Center for Theoretical Physics, Key Laboratory of Theoretical Physics of Gansu Province, Lanzhou University, Lanzhou 730000, China*

DERIVATION OF THE MASTER EQUATION

Consider N distant two-level systems (TLSs) interacting with a common squeezed reservoir confined in one-dimensional waveguide. Its Hamiltonian reads $\hat{H} = \hat{H}_S + \hat{H}_R + \hat{H}_I$ with ($\hbar = 1$)

$$\hat{H}_S = \sum_{i=1}^N \omega_0 \hat{\sigma}_i^\dagger \hat{\sigma}_i, \quad \hat{H}_R = \sum_k \omega_k \hat{a}_k^\dagger \hat{a}_k, \quad \hat{H}_I = \sum_{k,i} (g_{ki} \hat{a}_k + g_{ki}^* \hat{a}_k^\dagger) (\hat{\sigma}_i + \hat{\sigma}_i^\dagger). \quad (1)$$

Starting from the Liouville equation satisfied by the total system and tracing out the degrees of freedom of the reservoir, we obtain the master equation of the TLSs in the interaction picture under the Born-Markovian approximation [1] as

$$\dot{\tilde{\rho}}(t) = - \int_0^\infty d\tau \text{Tr}_R \{ [\hat{H}_I(t), [\hat{H}_I(t-\tau), \tilde{\rho}(t) \otimes R_0]] \}, \quad (2)$$

where $\tilde{\rho}(t) = e^{i\hat{H}_S t} \rho(t) e^{-i\hat{H}_S t}$, $\hat{H}_I(t) = e^{i(\hat{H}_S + \hat{H}_R)t} \hat{H}_I e^{-i(\hat{H}_S + \hat{H}_R)t}$, and $R_0 = \prod_k \hat{S}_k |0_k\rangle \langle 0_k| \hat{S}_k^\dagger$, with $\hat{S}_k = \exp[(\xi^* \hat{a}_k^2 - \xi \hat{a}_k^{\dagger 2})/2]$ and $\xi = re^{i\alpha}$, is the initial state of the squeezed reservoir. Introducing the notation $\hat{H}_I(t) \equiv \sum_i \hat{s}_i(t) \hat{\Gamma}_i(t)$ with $\hat{s}_i(t) = \hat{\sigma}_i^\dagger e^{i\omega_0 t} + \hat{\sigma}_i e^{-i\omega_0 t}$ and $\hat{\Gamma}_i(t) = \sum_k (g_{ki} \hat{a}_k e^{-i\omega_k t} + g_{ki}^* \hat{a}_k^\dagger e^{i\omega_k t})$, we obtain

$$\dot{\tilde{\rho}}(t) = - \sum_{i,j} \int_0^\infty d\tau \{ [\hat{s}_i(t) \hat{s}_j(t-\tau) \tilde{\rho}(t) - \hat{s}_j(t-\tau) \tilde{\rho}(t) \hat{s}_i(t)] \text{Tr}_R [\hat{\Gamma}_i(t) \hat{\Gamma}_j(t-\tau) R_0] + \text{h.c.} \}. \quad (3)$$

The correlation functions read

$$\text{Tr}_R [\hat{\Gamma}_i(t) \hat{\Gamma}_j(t-\tau) R_0] = \int_0^\infty d\omega \{ G_{ij}^-(\omega) [e^{-i\omega\tau} (\mathcal{N} + 1) + e^{i\omega\tau} \mathcal{N}] - G_{ij}^+(\omega) [\mathcal{M} e^{-i\omega(2t-\tau)} + \text{c.c.}] \}, \quad (4)$$

where $\mathcal{N} = \sinh^2 r$, $\mathcal{M} = \sqrt{\mathcal{N}(\mathcal{N} + 1)} e^{i\alpha}$, and $G_{ij}^-(\omega) = \sum_k g_{ki} g_{kj}^* \delta(\omega - \omega_k)$ and $G_{ij}^+(\omega) = \sum_k g_{ki} g_{kj} \delta(\omega - \omega_k)$. Here we have used the fact that both of $G_{ij}^\pm(\omega)$ are real functions for one-dimensional waveguide. Then Eq. (3) can be rewritten as

$$\begin{aligned} \dot{\tilde{\rho}}(t) = & - \sum_{i,j} \{ \mathcal{A}_{i,j} [(\hat{\sigma}_i^\dagger \hat{\sigma}_j^\dagger \tilde{\rho}(t) - \hat{\sigma}_j^\dagger \tilde{\rho}(t) \hat{\sigma}_i^\dagger) e^{i2\omega_0 t} + \hat{\sigma}_i \hat{\sigma}_j^\dagger \tilde{\rho}(t) - \hat{\sigma}_j^\dagger \tilde{\rho}(t) \hat{\sigma}_i] \\ & + \mathcal{B}_{i,j} [(\hat{\sigma}_i \hat{\sigma}_j \tilde{\rho}(t) - \hat{\sigma}_j \tilde{\rho}(t) \hat{\sigma}_i) e^{-i2\omega_0 t} + \hat{\sigma}_i^\dagger \hat{\sigma}_j \tilde{\rho}(t) - \hat{\sigma}_j \tilde{\rho}(t) \hat{\sigma}_i^\dagger] + \text{h.c.} \}. \end{aligned} \quad (5)$$

The utilization of $\int_0^\infty d\tau e^{-i(\omega \pm \omega_0)\tau} = \pi \delta(\omega \pm \omega_0) - i \frac{\mathcal{P}}{\omega \pm \omega_0}$ results in the defined $\mathcal{A}_{i,j}$ and $\mathcal{B}_{i,j}$ as

$$\begin{aligned} \mathcal{A}_{i,j} &= \int_0^\infty d\tau \int_0^\infty d\omega e^{-i\omega_0\tau} \{ G_{ij}^-(\omega) [e^{-i\omega\tau} (\mathcal{N} + 1) + e^{i\omega\tau} \mathcal{N}] - \sqrt{\mathcal{N}(\mathcal{N} + 1)} G_{ij}^+(\omega) [e^{-i\omega(2t-\tau)} e^{i\alpha} + \text{c.c.}] \} \\ &= \mathcal{N} \frac{\gamma_{ij}^-}{2} - \mathcal{M} \frac{\gamma_{ij}^+}{2} e^{-i2\omega_0 t} - i(\mathcal{N} + 1) \Delta_{ij}^+ + i\mathcal{N} \Delta_{ij}^- - i\mathcal{M} \Delta_{ij}'^- + i\mathcal{M}^* \Delta_{ij}'^+, \end{aligned} \quad (6)$$

$$\begin{aligned} \mathcal{B}_{ij} &= \int_0^\infty d\tau \int_0^\infty d\omega e^{i\omega_0\tau} \{ G_{ij}^-(\omega) [e^{-i\omega\tau} (\mathcal{N} + 1) + e^{i\omega\tau} \mathcal{N}] - \sqrt{\mathcal{N}(\mathcal{N} + 1)} G_{ij}^+(\omega) [e^{-i\omega(2t-\tau)} e^{i\alpha} + \text{c.c.}] \} \\ &= (\mathcal{N} + 1) \frac{\gamma_{ij}^-}{2} - \mathcal{M}^* \frac{\gamma_{ij}^+}{2} e^{i2\omega_0 t} + i\mathcal{N} \Delta_{ij}^+ - i(\mathcal{N} + 1) \Delta_{ij}^- - i\mathcal{M} \Delta_{ij}'^+ + i\mathcal{M}^* \Delta_{ij}'^-, \end{aligned} \quad (7)$$

where

$$\gamma_{ij}^\pm = 2\pi G_{ij}^\pm(\omega_0), \quad \Delta_{ij}^\pm = \mathcal{P} \int_0^\infty d\omega \frac{G_{ij}^-(\omega)}{\omega \pm \omega_0}, \quad \Delta_{ij}'^\pm = \mathcal{P} \int_0^\infty d\omega \frac{G_{ij}^+(\omega) e^{\pm i2\omega t}}{\omega \pm \omega_0}. \quad (8)$$

The neglect of the rapidly oscillating terms in the master equation under the secular approximation [2] converts Eq. (5) into

$$\begin{aligned}\dot{\tilde{\rho}}(t) = & \sum_{i,j} \{i(\mathcal{N}+1)[\Delta_{ij}^+(\hat{\sigma}_i\hat{\sigma}_j^\dagger\tilde{\rho}(t) - \tilde{\rho}(t)\hat{\sigma}_j\hat{\sigma}_i^\dagger) + \Delta_{ij}^-(\hat{\sigma}_i^\dagger\hat{\sigma}_j\tilde{\rho}(t) - \tilde{\rho}(t)\hat{\sigma}_j^\dagger\hat{\sigma}_i)] \\ & - i\mathcal{N}[\Delta_{ij}^+(\hat{\sigma}_i^\dagger\hat{\sigma}_j\tilde{\rho}(t) - \tilde{\rho}(t)\hat{\sigma}_j^\dagger\hat{\sigma}_i) + \Delta_{ij}^-(\hat{\sigma}_i\hat{\sigma}_j^\dagger\tilde{\rho}(t) - \tilde{\rho}(t)\hat{\sigma}_j\hat{\sigma}_i^\dagger)] \\ & + \gamma_{ij}^-/2[\mathcal{N}\check{\mathcal{D}}_{\hat{\sigma}_i^\dagger, \hat{\sigma}_j} + (\mathcal{N}+1)\check{\mathcal{D}}_{\hat{\sigma}_i, \hat{\sigma}_j^\dagger}] - \gamma_{ij}^+/2[\mathcal{M}\check{\mathcal{D}}_{\hat{\sigma}_i^\dagger, \hat{\sigma}_j} + \mathcal{M}^*\check{\mathcal{D}}_{\hat{\sigma}_i, \hat{\sigma}_j^\dagger}]\tilde{\rho}(t)\},\end{aligned}\quad (9)$$

where $\check{\mathcal{D}}_{\hat{A}, \hat{B}} \equiv 2\hat{A} \cdot \hat{B} - \hat{B}\hat{A} - \hat{B}\hat{A}$. According to the commutation relation $[\hat{\sigma}_i^\dagger, \hat{\sigma}_j] = \hat{\sigma}_i^z\delta_{i,j}$ and $\hat{\sigma}_i^\dagger\hat{\sigma}_i = (1 + \hat{\sigma}_i^z)/2$, we have

$$\Delta_{ij}^+(\hat{\sigma}_i\hat{\sigma}_j^\dagger\tilde{\rho}(t) - \tilde{\rho}(t)\hat{\sigma}_j\hat{\sigma}_i^\dagger) + \Delta_{ij}^-(\hat{\sigma}_i^\dagger\hat{\sigma}_j\tilde{\rho}(t) - \tilde{\rho}(t)\hat{\sigma}_j^\dagger\hat{\sigma}_i) = \frac{\Delta_{ij}^+ + \Delta_{ij}^-}{2}[\hat{\sigma}_i^\dagger\hat{\sigma}_j + \hat{\sigma}_i\hat{\sigma}_j^\dagger, \tilde{\rho}(t)] + (\Delta_{ii}^- - \Delta_{ii}^+)[\hat{\sigma}_i^\dagger\hat{\sigma}_i, \tilde{\rho}(t)],\quad (10)$$

$$\Delta_{ij}^+(\hat{\sigma}_i^\dagger\hat{\sigma}_j\tilde{\rho}(t) - \tilde{\rho}(t)\hat{\sigma}_j^\dagger\hat{\sigma}_i) + \Delta_{ij}^-(\hat{\sigma}_i\hat{\sigma}_j^\dagger\tilde{\rho}(t) - \tilde{\rho}(t)\hat{\sigma}_j\hat{\sigma}_i^\dagger) = \frac{\Delta_{ij}^+ + \Delta_{ij}^-}{2}[\hat{\sigma}_i^\dagger\hat{\sigma}_j + \hat{\sigma}_i\hat{\sigma}_j^\dagger, \tilde{\rho}(t)] - (\Delta_{ii}^- - \Delta_{ii}^+)[\hat{\sigma}_i^\dagger\hat{\sigma}_i, \tilde{\rho}(t)].\quad (11)$$

Finally, we arrive at

$$\dot{\tilde{\rho}}(t) = -i[\Delta_{\mathcal{N}} \sum_i \hat{\sigma}_i^\dagger\hat{\sigma}_i + \hat{H}_{\text{DD}}, \tilde{\rho}] + \sum_{i,j} \{\gamma_{ij}^-/2[\mathcal{N}\check{\mathcal{D}}_{\hat{\sigma}_i^\dagger, \hat{\sigma}_j} + (\mathcal{N}+1)\check{\mathcal{D}}_{\hat{\sigma}_i, \hat{\sigma}_j^\dagger}] - \gamma_{ij}^+/2[\mathcal{M}\check{\mathcal{D}}_{\hat{\sigma}_i^\dagger, \hat{\sigma}_j} + \mathcal{M}^*\check{\mathcal{D}}_{\hat{\sigma}_i, \hat{\sigma}_j^\dagger}]\}\tilde{\rho}(t),\quad (12)$$

where $\Delta_{\mathcal{N}} = (2\mathcal{N}+1)(\Delta_{ii}^+ - \Delta_{ii}^-)$ and $\hat{H}_{\text{DD}} = -\sum_{i,j} \Delta_{ij}(\hat{\sigma}_i^\dagger\hat{\sigma}_j + \hat{\sigma}_i\hat{\sigma}_j^\dagger)/2$ with $\Delta_{ij} = \Delta_{ij}^+ + \Delta_{ij}^-$.

RECTANGULAR HOLLOW METAL WAVEGUIDE

When the waveguide is formed by a rectangular hollow metal, the electromagnetic modes in the waveguide are the transverse modes TE_{mn} and TM_{mn} with the cutoff frequency $\omega_{mn} = c[(m\pi/a)^2 + (n\pi/b)^2]^{1/2}$, where a, b are the transverse lengths of the waveguide, and m, n are non-negative integers. Their dispersion relations are $\omega_k^{mn} = [(ck)^2 + \omega_{mn}^2]^{1/2}$ with k being the longitudinal wave number and c being the speed of light. Considering the dominate mode $m = n = 1$ under the condition that the TLSs are polarized in the z direction ($\mathbf{d}_i = d\mathbf{e}_z$), we can calculate the spectral densities as [3]

$$G_{ij}^\pm(\omega) = \frac{\Gamma_{11}}{2\pi} \frac{\cos[k(z_i \pm z_j)]}{[(\omega/\omega_{11})^2 - 1]^{1/2}} \Theta(\omega - \omega_{11})\quad (13)$$

with $\Theta(\omega - \omega_{11})$ being the Heaviside step function, $\Gamma_{11} = 4\omega_{11}\tilde{u}_{11,i}\tilde{u}_{11,j}/(\epsilon_0 cab)$, and $\tilde{u}_{11,i} = d\sin(\frac{\pi}{a}x_i)\sin(\frac{\pi}{b}y_i)$. In the following, we calculate the dipole-dipole coupling strength. The substitution of Eq. (13) into the definition of Δ_{ij} , we have

$$\Delta_{ij} = \frac{\Gamma_{11}}{2\pi} \mathcal{P} \int_{\omega_{11}}^{+\infty} \frac{\cos(kz_{ij})}{\sqrt{(\omega/\omega_{11})^2 - 1}} \frac{1}{\omega^2 - \omega_0^2} d\omega = \frac{\Gamma_{11}}{2\pi} \mathcal{P} \int_{-\infty}^{+\infty} \frac{\exp(i\omega_{11}z_{ij}x/c)}{x^2 + 1 - \omega_0^2/\omega_{11}^2} dx.\quad (14)$$

where $z_{ij} \equiv |z_i - z_j|$ and $x \equiv \sqrt{(\omega/\omega_{11})^2 - 1}$. Making an analytical extension of x to a complex variable and drawing a contour to encircle the upper half complex plane (see Fig. 1), we, according to Cauchy's residue theorem [4], obtain

$$\Delta_{ij} = \frac{\Gamma_{11}}{2\pi} [2\pi i \sum_{\text{Inside the contour}} \text{Res}(\text{poles}) + \pi i \sum_{\text{Real axis}} \text{Res}(\text{simple poles})],\quad (15)$$

where $\text{Res}(\cdot)$ denotes the residue contributed from different kinds of poles. Focusing on $\omega_0 > \omega_{11}$, we can see that Eq. (14) has only two simple poles $x_\pm = \pm\sqrt{\omega_0^2/\omega_{11}^2 - 1}$ in real axis. Then, we have $\Delta_{ij} = \frac{i\Gamma_{11}}{2} \sum_{i=\pm} \text{Res}(x_i)$. It can be readily evaluated the residues $\text{Res}(x_\pm) = \pm \exp(\pm i\sqrt{\omega_0^2 - \omega_{11}^2}z_{ij}/c)/(2\sqrt{\omega_0^2/\omega_{11}^2 - 1})$. Therefore, we have

$$\Delta_{ij} = -[\Gamma\zeta\omega_{11}/(2c)] \sin(z_{ij}/\zeta),\quad (16)$$

where $\zeta = c(\omega_0^2 - \omega_{11}^2)^{-1/2}$. On the other hand, it is natural to obtain

$$\gamma_{ij}^\pm = 2\pi G_{ij}^\pm(\omega_0) = (\Gamma_{11}\zeta\omega_{11}/c) \cos[(z_i \pm z_j)/\zeta].\quad (17)$$

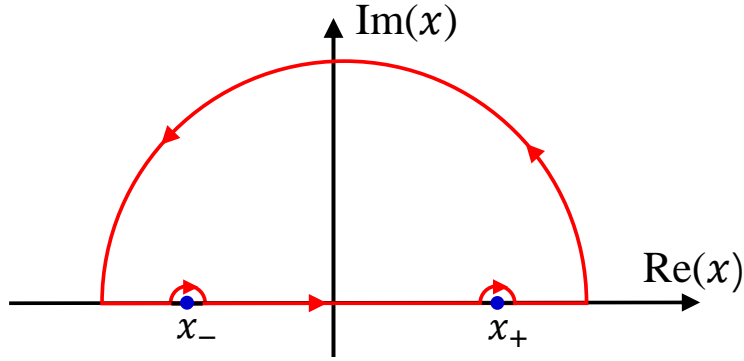


FIG. 1. Path of the contour integration in the complex plane $\text{Re}(x) + i\text{Im}(x)$ for the calculation of Δ_{ij} .

It is interesting to see that we can change the phase difference between Δ_{ij} and γ_{ij}^\pm to switch on or off one of them by controlling the positions of TLSs. If their positions satisfy $z_i \pm z_j = 2n_\pm \pi \zeta$ with n_\pm being integers, then we have $\Delta_{ij} = 0$ and $\gamma_{ij}^\pm = \Gamma_{11} \zeta \omega_{11} / c \equiv A$. The master equation (12) turns to

$$\dot{\tilde{\rho}}(t) = -i[\Delta_N \hat{S}^z, \tilde{\rho}(t)] + A/2[\mathcal{N} \check{\mathcal{D}}_{\hat{S}+, \hat{S}-} + (\mathcal{N} + 1) \check{\mathcal{D}}_{\hat{S}-, \hat{S}+} - \mathcal{M} \check{\mathcal{D}}_{\hat{S}+, \hat{S}+} - \mathcal{M}^* \check{\mathcal{D}}_{\hat{S}-, \hat{S}-}] \tilde{\rho}(t), \quad (18)$$

where $\hat{S}^z \equiv \sum_i (\hat{\sigma}_i^\dagger \hat{\sigma}_i - 1/2)$ and $\hat{S}^\pm = \sum_i \sigma_i^\pm$.

THE STEADY STATE

The master equation (18) can be written as

$$\dot{\tilde{\rho}}(t) = -i\Delta_N [\hat{S}_z, \tilde{\rho}(t)] + \frac{A}{2} [\mathcal{N} \check{\mathcal{D}}_{\hat{S}+, \hat{S}-} + (\mathcal{N} + 1) \check{\mathcal{D}}_{\hat{S}-, \hat{S}+} + |\mathcal{M}| (\check{\mathcal{D}}_{\hat{S}+, \hat{S}+} + \check{\mathcal{D}}_{\hat{S}-, \hat{S}-})] \tilde{\rho}(t), \quad (19)$$

where $\hat{S}_\pm = \hat{S}^\pm e^{\pm i \frac{\alpha \pm \pi}{2}}$. After introducing

$$\hat{R}_z = (4|\mathcal{M}|)^{-1/2} (\hat{S}_+ \sinh r + \hat{S}_- \cosh r), \quad (20)$$

$$\hat{R}_\pm = \pm (4|\mathcal{M}|)^{-1/2} (\hat{S}_+ \sinh r - \hat{S}_- \cosh r) - \hat{S}_z, \quad (21)$$

we can recast Eq. (19) into

$$\dot{\tilde{\rho}}(t) = i\Delta_N / 2 [\hat{R}_+ + \hat{R}_-, \tilde{\rho}(t)] + 2A|\mathcal{M}| \check{\mathcal{D}}_{\hat{R}_z, \hat{R}_z^\dagger} \tilde{\rho}(t). \quad (22)$$

It is easy to verify the following commutation relations [5]

$$[\hat{R}_+, \hat{R}_-] = 2\hat{R}_z, \quad [\hat{R}_z, \hat{R}_\pm] = \pm \hat{R}_\pm, \quad (23)$$

$$[\hat{R}_+^\dagger, \hat{R}_-^\dagger] = -2\hat{R}_z^\dagger, \quad [\hat{R}_z^\dagger, \hat{R}_\pm^\dagger] = \mp \hat{R}_\pm^\dagger. \quad (24)$$

The eigenvectors of the non-Hermitian operator \hat{R}_z and its Hermitian conjugate operator \hat{R}_z^\dagger , i.e., $\hat{R}_z |\psi_m\rangle = m |\psi_m\rangle$ and $\hat{R}_z^\dagger |\phi_m\rangle = m |\phi_m\rangle$, form a complete set of biorthogonal basis.

$$\sum_m |\psi_m\rangle \langle \phi_m| = \sum_m |\phi_m\rangle \langle \psi_m| = \mathbb{I}, \quad \langle \phi_m | \psi_n \rangle = \delta_{m,n}. \quad (25)$$

It can be calculated that

$$|\psi_m\rangle = e^{i\vartheta \hat{S}_z} e^{-\frac{\pi}{4}(\hat{S}_+ - \hat{S}_-)} |j, m\rangle. \quad (26)$$

$$|\phi_m\rangle = e^{-i\vartheta \hat{S}_z} e^{-\frac{\pi}{4}(\hat{S}_+ - \hat{S}_-)} |j, m\rangle, \quad (27)$$

with $j = N/2, m = -N/2, -N/2 + 1, \dots, N/2$, and $\vartheta = \ln \sqrt{\tanh r}$. According to the commutation relations (23) and (24), we have

$$\hat{R}_\pm |\psi_m\rangle = \sqrt{(j \mp m)(j \pm m + 1)} |\psi_{m\pm 1}\rangle, \quad (28)$$

$$\hat{R}_\mp^\dagger |\phi_m\rangle = \sqrt{(j \mp m)(j \pm m + 1)} |\phi_{m\pm 1}\rangle. \quad (29)$$

We expand $\tilde{\rho}(t)$ in the biorthogonal basis as

$$\tilde{\rho}(t) = \sum_{m,n=-j}^j \rho_{mn}(t) |\psi_m\rangle\langle\psi_n|, \quad (30)$$

with $\rho_{mn}(t) = \langle\phi_m|\tilde{\rho}(t)|\phi_n\rangle$. Rewriting $\hat{R}_z^\dagger = (4|\mathcal{M}|)^{-1/2}[\hat{R}_+ - \hat{R}_- + 2\cosh(2r)\hat{R}_z]$, we have

$$\hat{R}_z^\dagger |\psi_m\rangle = \frac{1}{\sqrt{4|\mathcal{M}|}} [\sqrt{(j-m)(j+m+1)} |\psi_{m+1}\rangle - \sqrt{(j+m)(j-m+1)} |\psi_{m-1}\rangle + 2m \cosh(2r) |\psi_m\rangle]. \quad (31)$$

Using Eqs. (21) and (31), we convert Eq. (22) into

$$\begin{aligned} \langle\phi_k|\dot{\tilde{\rho}}(t)|\phi_{k'}\rangle &= \left\{ Ac_{kk'}(t) \langle\phi_k|\phi_{k'}\rangle k [k' \sinh(2r) - k \cosh(2r)] + \frac{i\Delta_{\mathcal{N}} - A(k-1)}{2} c_{k-1,k'}(t) \langle\phi_{k-1}|\phi_{k'}\rangle \sqrt{(j+k)(j-k+1)} \right. \\ &\quad \left. + \frac{i\Delta_{\mathcal{N}} + A(k+1)}{2} c_{k+1,k'}(t) \langle\phi_{k+1}|\phi_{k'}\rangle \sqrt{(j-k)(j+k+1)} \right\} + \text{H.c.}, \end{aligned} \quad (32)$$

where we have defined $\tilde{\rho}_{mn}(t) = c_{mn}(t) \langle\phi_m|\phi_n\rangle$. Using Eq. (29), one can prove

$$\langle\phi_{k-1}|\phi_{k'}\rangle \sqrt{(j+k)(j-k+1)} = \langle\phi_k|\hat{R}_+|\phi_{k'}\rangle = [k' \sinh(2r) - k \cosh(2r)] \langle\phi_k|\phi_{k'}\rangle - \langle\phi_k|\hat{S}_z|\phi_{k'}\rangle, \quad (33)$$

$$\langle\phi_{k+1}|\phi_{k'}\rangle \sqrt{(j-k)(j+k+1)} = \langle\phi_k|\hat{R}_-|\phi_{k'}\rangle = [k \cosh(2r) - k' \sinh(2r)] \langle\phi_k|\phi_{k'}\rangle - \langle\phi_k|\hat{S}_z|\phi_{k'}\rangle, \quad (34)$$

where $\hat{R}_\pm = \mp \cosh(2r)\hat{R}_z \pm \sinh(2r)\hat{R}_z^\dagger - \hat{S}_z$ derived from Eqs. (20) and (21) have been used. The substitution of Eqs. (33) and (34) into Eq. (32) results in

$$\begin{aligned} \langle\phi_k|\dot{\tilde{\rho}}(t)|\phi_{k'}\rangle &= \frac{\langle\phi_k|\phi_{k'}\rangle}{2} [k' \sinh(2r) - k \cosh(2r)] \{ [i\Delta_{\mathcal{N}} - A(k-1)] c_{k-1,k'}(t) - [i\Delta_{\mathcal{N}} + A(k+1)] c_{k+1,k'}(t) \\ &\quad + 2Ak c_{kk'}(t) \} - \frac{\langle\phi_k|\hat{S}_z|\phi_{k'}\rangle}{2} \{ [i\Delta_{\mathcal{N}} - A(k-1)] c_{k-1,k'}(t) + [i\Delta_{\mathcal{N}} + A(k+1)] c_{k+1,k'}(t) \} + \text{H.c.} \end{aligned} \quad (35)$$

The steady-state equation requires $\langle\phi_k|\dot{\tilde{\rho}}(t)|\phi_{k'}\rangle = 0$. It is satisfied by

$$[i\Delta_{\mathcal{N}} + A(k+1)] c_{k+1,k'} = (Ak - i\Delta_{\mathcal{N}}) c_{k,k'}, \quad [i\Delta_{\mathcal{N}} - A(k-1)] c_{k-1,k'} = -(Ak + i\Delta_{\mathcal{N}}) c_{k,k'}, \quad (36)$$

where $\langle\phi_{k'}|\hat{S}_z|\phi_k\rangle = \langle\phi_k|\hat{S}_z|\phi_{k'}\rangle$ has been used. Due to the independence of k' in Eq. (36), the variables in the steady-state solution $c_{k,k'}$ can be separated as $c_{k,k'} = p_k q_{k'}$, where $q_k = p_k^*$. Then we obtain

$$[A(k+1) + i\Delta_{\mathcal{N}}] p_{k+1} = (Ak - i\Delta_{\mathcal{N}}) p_k. \quad (37)$$

The combination of the normalization condition with this recurrence relation (37) can give the final result of the steady state.

* anjhong@lzu.edu.cn

- [1] Heinz-Peter Breuer and Francesco Petruccione, *The Theory of Open Quantum Systems* (Oxford University Press, Oxford, 2007).
- [2] H. Mäkelä and M. Möttönen, “Effects of the rotating-wave and secular approximations on non-Markovianity,” *Phys. Rev. A* **88**, 052111 (2013).
- [3] Ephraim Shahmoon and Gershon Kurizki, “Nonradiative interaction and entanglement between distant atoms,” *Phys. Rev. A* **87**, 033831 (2013).
- [4] Sadri Hassani, *Mathematical Physics: A Modern Introduction to Its Foundations*, 2nd ed. (Springer International Publishing, New York, 2013).
- [5] G. S. Agarwal and R. R. Puri, “Cooperative behavior of atoms irradiated by broadband squeezed light,” *Phys. Rev. A* **41**, 3782–3791 (1990).